Physica A 517 (2019) 385–391

Contents lists available at ScienceDirect

Physica A

journal homepage: www.elsevier.com/locate/physa

SANS study of Amyloid β_{1-40}: Unfolded monomers in DMSO, multidimensional aggregates in water medium

Giulia Festa [a], Giulia Sancesario [b,c], Carmelo Corsaro [d,*], Sveva Longo [d], Domenico Mallamace [d], Enza Fazio [d], Laura Arcidiacono [a], Victoria Garcia Sakai [e], Roberto Senesi [a,f,**], Giuseppe Sancesario [g], Francesco Mallamace [d,h], Carla Andreani [a,f]

[a] CENTRO FERMI - Museo Storico della Fisica e Centro Studi e Ricerche "Enrico Fermi", 00184 Rome, Italy
[b] Universitá degli Studi di Roma "Tor Vergata", Department of Experimental Medicine and Surgery, 00133 Rome, Italy
[c] IRCCS Fondazione Santa Lucia, Rome, Italy
[d] MIFT Department, University of Messina, 98166 Messina, Italy
[e] Science and Technology Facilities Council, ISIS Pulsed Neutron and Muon source, UK
[f] Universitá degli Studi di Roma "Tor Vergata", NAST Centre and Department of Physics, 00133 Rome, Italy
[g] Universitá degli Studi di Roma "Tor Vergata", Department of Systems Medicine, 00133 Rome, Italy
[h] NSE Department, Massachusetts Institute of Technology, Cambridge, MA 02139, USA

HIGHLIGHTS

- The size of the three forms of amyloid beta peptides as well as their fractal nature are measured at physiologic conditions.
- Small Angle Neutron Scattering allows to clearly distinguish monomer, oligomer and fibril preparations.
- Open and compact structures of the peptide are detected, that correspond to the monomeric and fibril states.

ARTICLE INFO

Article history:
Received 9 July 2018
Received in revised form 12 October 2018
Available online 14 November 2018

Keywords:
SANS
Amyloid fibrils
Amyloid aggregation

ABSTRACT

Neurodegenerative diseases such as Alzheimer's are characterized by neuritic plaques throughout the brain gray matter, associated with neurofibrillary tangles and neuron loss. These plaques are formed by abnormal aggregation of amyloid beta ($A\beta$) peptide into insoluble fibrils. In the present work we study the $A\beta_{1-40}$ peptide in the three aggregations states – monomers, oligomers and fibrils – via small angle neutron scattering (SANS) technique. The size of the three forms as well as their fractal nature are investigated at physiologic conditions. Our results evidence that the $A\beta_{1-40}$ peptide has a good aggregation capability but can also adopt an unfolded conformation in particular conditions, as for example, when incubated in DMSO.

1. Introduction

Alzheimer's disease (AD) is histologically characterized by innumerable neuritic plaques throughout the brain's gray matter, associated with neurofibrillary tangles and neuron loss [1]. Amyloid β ($A\beta$) peptides, involved in the pathogenesis

* Corresponding author at: MIFT Department, University of Messina, 98166 Messina, Italy.
** Corresponding author at: Universitá degli Studi di Roma "Tor Vergata", NAST Centre and Department of Physics, 00133 Rome, Italy.
E-mail addresses: roberto.senesi@uniroma2.it (R. Senesi), ccorsaro@unime.it (C. Andreani).

https://doi.org/10.1016/j.physa.2018.11.027
0378-4371/

of Alzheimer's disease, are physiological derivatives of the amyloid precursor protein (APP), a single-pass transmembrane protein expressed at high levels in the normal brain. [1] After APP proteolysis, Aβ peptides of 36–43 amino acids are released from neural cells extracellularly in the interstitial fluid and cleared out in the blood stream, remaining in the cerebrospinal fluid at very low (pg/ml) concentrations. [2] Although many questions remain unsolved about the importance of plaques in the pathogenesis of AD, actually the abnormal accumulation of neuritic plaques in various areas of the brain in AD precedes and over time is invariably associated to the neurodegeneration. [3,4] Moreover, in the elderly with dementia in the interstitial spaces to form soluble oligomers and insoluble fibrils that precipitate in amyloid plaques and lead to tissue damage. [5] Why Aβ peptides aggregate and accumulate in the brains of elderly individuals is unclear but it could relate to changes in Aβ molecule biophysical characteristics. [6,7] The aggregation process cannot be studied on native Aβ peptides in biological fluid because of their low pg/ml concentration, so that synthetic Aβ peptides are commonly used *in vitro*. However, *in vitro* we can just investigate the biophysical characteristics of Aβ in different experimental conditions, trying to translate results and find suggestions that are clinically relevant. In fact, we can hardly reproduce the aggregation processes of Aβ occurring in human brains *in vitro*: indeed, *in vitro* the formation of Aβ aggregates is dependent on concentration above a critical level defined approximately at 100 μg/ml that is much higher than in biological fluids; [8] moreover, Aβ monomers are not easily dissolved in water [9–11], so that organic solvents are commonly used, particularly fluorinated alcohols, such as trifluoroethanol (TFE) or hexafluoroisopropanol (HFIP), and the highly polar organic liquid dimethyl sulfoxide (DMSO). In the former, Aβ peptides do not aggregate and have predominantly α-helix conformations, in contrast to what happens in DMSO. [8–13] In a recent paper, the Aβ monomer structural variations affected by water and DMSO were analyzed using an all-atom molecular dynamic (MD) simulation: under water condition, the Aβ_{1-42} protein monomers folded into α-helices and β-strands, whereas under DMSO, Aβ_{1-42} lost α-helix conformations with the generation of unfolded structures. [13] Such an action of DMSO may be therapeutically relevant, since DMSO at low doses in vivo improves cognitive function and prevents Aβ synaptotoxicity in a preclinical Alzheimer's disease model. While DMSO has a widespread use so far as a vehicle for water-insoluble therapeutic drugs, these data suggest that DMSO itself may also exert a bioactive beneficial effect to counteract Alzheimer's disease pathology. [14] Therefore, it would be interesting to study in further detail the Aβ conformational changes induced by DMSO. Small angle neutron scattering (SANS) is a promising nondestructive technique to investigate Aβ peptide aggregation in solution. Typically, small angle scattering is used to determine the size or shape of large aggregates during aggregation. Instead, Zhang-Haagen et al. showed that SANS is able to resolve monomers of small molecular weight such as Aβ in deuterated HFIP, of a radius of gyration of 1.0 $\pm$ 0.1 nm (in agreement with 3D NMR). [15] To evaluate the possibilities and limitations of SANS technique to observe size and conformational characteristics of Aβ, we evaluated Aβ_{1-40}, the most common Aβ peptide, in disparate solvents. Since water (H_2O or D_2O buffers) can induce fast aggregation of monomer while DMSO can disaggregate Aβ oligomers/fibrils, we examined Aβ_{1-40} monomeric solution in DMSO, and Aβ_{1-40} oligomer and protofibril preparations in biological relevant environment (D_2O buffers). Using separate and stable samples of monomers, and oligomer/fibril preparations of Aβ_{1-40}, may help to avoid interferences and masking of clear signals arising instead from samples containing mixtures of Aβ monomers and aggregates. We compared the performance of SANS and SDS–PAGE techniques for the determination of Aβ_{1-40} aggregate size, identifying monomers, oligomers and fibrils. [11,16,17] Finally, SANS allows us to obtain information about the fractal nature and conformational features of the different revealed aggregates.

2. Materials and methods

2.1. Materials

Synthetic Aβ_{1-40} peptides were purchased from Anaspec (Fremont, CA). Aggregates of Aβ_{1-40} are obtained by using the Dahlgren's modification of Lambert's protocol [18], as previously reported [19]. Briefly, Aβ_{1-40} monomers (6 mg) were dissolved in anhydrous dimethyl sulfoxide to 5 mM and sonicated for 10 min. Thereafter, the corresponding monomeric Aβ solutions were diluted to 2 mg/ml either in cold HAM's-F12 culture medium (Euroclone) and incubated overnight at 4 °C for oligomer formation, or in HCl 10 mM and incubated at 37 °C overnight for fibril formation. All samples were dehydrated and resuspended in 1 ml of D_2O just before the SANS experiment. Preliminary measurements were performed through the gel electrophoresis technique called SDS–PAGE. [20] SDS–PAGE analysis without heat denaturation, followed by silver staining was assessed to confirm the formation of Aβ aggregates. Monomers and aggregated forms corresponding to an original content of 1 μg of monomers for each sample, were run in 16% SDS–PAGE tris-tricine buffer. After the runs, gels were fixed in 40% methanol and 10% acetic acid overnight, and then were silver stained (Bio-Rad Silver Stain kit). A molecular weight protein marker was used for reference (BenchMark Pre-stained Protein Ladder, Invitrogen).

2.2. Methods

Small angle neutron scattering (SANS) [21] experiments are performed at the SANS2D beamline [22,23] of the Science and Technology Facilities Council - ISIS Spallation Neutron and Muon Source. The SANS2D beamline is dedicated to the study of size, shape, internal structure and spatial arrangement in nanomaterials, "soft matter", and colloidal systems, including those of biological origin, on length scales between 0.24–300 nm. [21] This beamline has a wide Q-range ($0.02 < Q\ nm^{-1} < 20$): five of 2 m guide sections with variable collimation apertures and two moveable 1 m^2 detectors provide the biggest

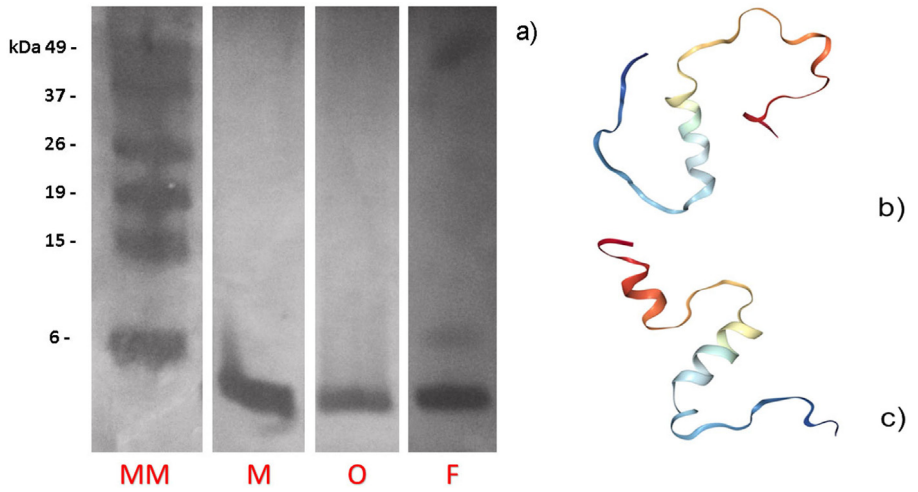

Fig. 1. (a) Silver stain of synthetic aggregates and monomers of Aβ_{1-40} peptide. MM= Molecular Marker; M= Monomers, O= Oligomers, F= Fibrils. All the preparations show the band of the basic Aβ_{1-40} peptide unit at $\simeq$ 4 kDa and different aggregates. (b) A partially folded structure of Aβ_{1-40} in an aqueous environment [PDB code 2LFM], (c) a conformational structure of Aβ_{1-40} monomers with two α-helices induced by the presence of trifluoroethanol [PDB code 1AML]. See main text for details.

detector area of any SANS instrument in the world that is almost 77,000 pixels. SANS2D has a high-flux at sample position and small size/volume samples of less than 15 mm diameter or only 0.3–3 ml can be analyzed. The instrument is equipped with the sample environment system that control, experimental conditions such as temperature and pressure. In the present study, quartz cuvettes were used and positioned in a thermostat double-deck sample changer at 37 °C to better simulate the physiological temperatures. [24] Samples of Aβ_{1-40} monomers, oligomers and fibrils are prepared with a concentration of 2 mg/ml and loaded into 2 mm path length 'tank' cuvettes for the largest beam size possible to improve the signal/background ratio. These proteins are unstable for a synchrotron X-ray beam and, in general, their stability at physiological temperature is not more than 10 h. We stress that the samples are warmed to 37 °C to simulate physiological conditions and study the effective aggregation state of the Aβ_{1-40} peptide. Each sample was measured for 2 h and measurements repeated 3 times. We find no differences among the different experiments so we averaged the corresponding runs to improve the statistics. Data processing and reduction was performed by using the Mantid application. [25]

3. Results and discussion

The formation of aggregates of Aβ_{1-40} is confirmed by running all samples in SDS/PAGE, followed by silver staining. All samples show the band of the basic Aβ_{1-40} peptide unit at about 4 kDa and different aggregates with increasing dimensions going towards the fibril systems (see Fig. 1). In panels b and c of Fig. 1 two different conformations of the Aβ_{1-40} peptide in two different solutions are reported. These conformations were extracted by the Protein Data Bank database (https://www.rcsb.org/) and correspond to an aqueous environment (panel b, PDB code 2LFM) and to a 40% (by vol.) trifluoroethanol/water solution (panel c, PDB code 1AML). It is noteworthy that depending on the solvent the peptide can adopt different conformations with one or two α-helices. In particular, in aqueous environment the monomer possesses only one α-helix (panel b of Fig. 1) whereas the presence of trifluoroethanol favors the formation of two α-helices (panel c of Fig. 1). Furthermore, as mentioned, when diluted in HFIP monomers do not aggregate.

The coherent contribution of the intensity scattered by N particles in a solution of volume V can be written as:

$$I(Q) = \frac{N}{V} S(Q) F(Q) + bkg \tag{1}$$

where *bkg* is the background signal and takes into account the solvent contribution to the signal and the incoherent scattering. The Structure factor S(Q) equals 1 for low concentrations as in our case and the Form factor F(Q) depends on the shape and size of the scattering objects but not on the concentration. The data analysis was carried out by using a geometry independent Form factor known as the Becauge model [15,26]:

$$F(Q) = G \exp\left(\frac{-Q^2 R_g^2}{3}\right) + \left(\frac{C}{Q^d}\right)\left[erf\left(\frac{QR_g}{\sqrt{6}}\right)\right]^{3d} \tag{2}$$

where

$$C = \left(\frac{Gd}{R_g^d}\right)\left[\frac{6d^2}{(2+d)(2+2d)}\right]^{d/2} \Gamma\left(\frac{d}{2}\right) \tag{3}$$

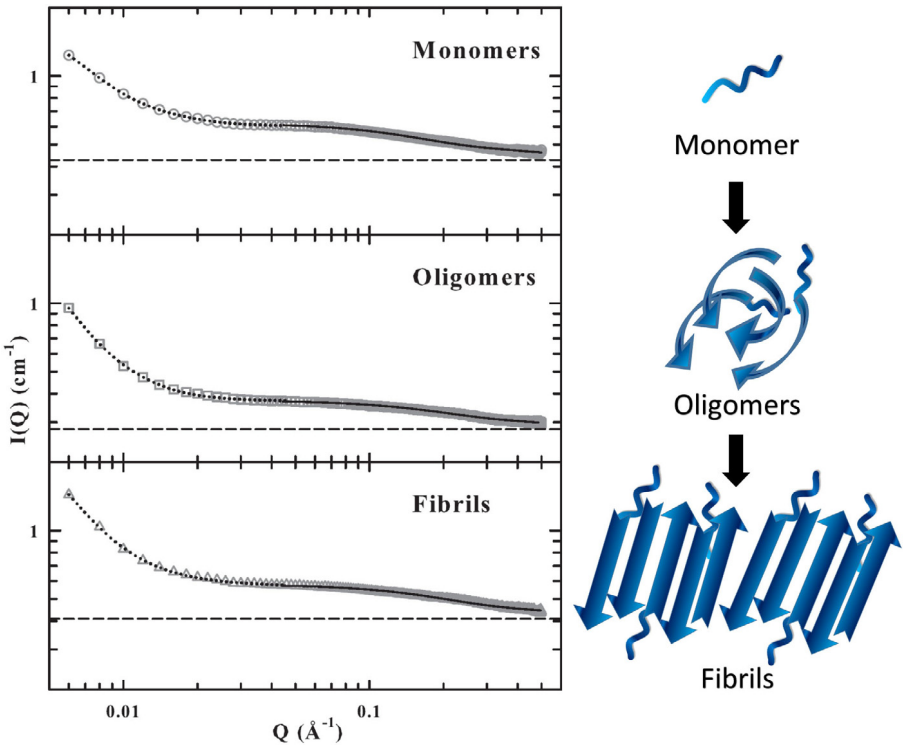

Fig. 2. Left side — Best fit of the SANS spectra for monomers (top), oligomers (middle) and fibrils (bottom) of Aβ_{1-40} peptide by using the Becauge model in two wave-vector regimes. The signal of the aggregate is analyzed (dotted lines) at low Q (Q <0.045 Å^{-1}) whereas that of the basic unit (solid lines) at high Q (0.045 <Q <0.5 Å^{-1}). The dashed lines represent the background value obtained by fitting the high-Q data. Right side — schematic structure of monomer, oligomers and fibrils.

with G as the Guinier scale factor, C as the Porod scale factor and d as the Porod exponent that corresponds to the dimensionality (d=2 is a Gaussian coil). R_g is the radius of gyration which provides an estimate of the particle size and is related to the hydrodynamic radius (RH) by R_g = 0.774 RH. The issue of considering the Porod and Guinier scaling factor, G and C respectively, was separately is known to produce artifacts during the data analysis [27]. We used the model in its complete and correct form and the data analysis is performed in two different wave vector regions (Q <0.045 Å^{-1}; 0.045 <Q <0.5 Å^{-1}) because, as suggested by the SDS/PAGE analysis, the system consists of two phases. In particular, the basic unit, that is the monomer, is always present (and detectable in the high-Q region, see Fig. 2) together with the corresponding aggregate state of dimensions gradually increasing from oligomers to fibrils. The signal of the aggregate state is indeed detectable in the low-Q region of the SANS spectra.

Fig. 2 reports the SANS data recorded for the three considered systems together with the best-fit obtained by using the Becauge model (Eqs. (1) and (2)) in two wave-vector regimes. As mentioned, the signal of the aggregate is analyzed (dotted lines) at low Q (Q <0.045 Å^{-1}) whereas that of the basic unit (solid lines) at high Q (0.045 <Q <0.5 Å^{-1}). The dashed lines represent the background value obtained by fitting the high-Q data. By looking at the fit parameters listed in Table 1, one can easily note that in the high-Q region, the radius R_g of the basic unit, the monomer, is of the order of 10 Å as reported in literature. [11] However, oligomers and fibrils show in this Q-region a value of R_g that is even slightly lower than that of monomers. This can be justified by the presence of a higher-density surface layer [15] and can suggest that the structure of the basic unit in the monomeric solution is more open (unfolded) with respect to that in oligomer and fibril systems. From the low-Q regions, we find that the oligomers have an average dimension of order of 378 ± 41 Å corresponding to medium size oligomers. [11] Fibrils have dimensions of about 706 ± 52 Å, almost twice those of oligomers. For what concerns the exponent d in the low-Q region, it has values between 2.44 ± 0.06 and 3.1 ± 0.1 corresponding to collapsed chains, while for all samples it is about 1.3 in the high-Q region indicating open chains. [26] Finally, the value of the Guinier scaling factor G for monomers is 1.30 ± 0.07 cm^{-1}, for oligomers is 2.5 ± 0.6 cm^{-1} and for fibrils is 12 ± 1 cm^{-1} in the low-Q, region confirming an increase in the size of the scattering object and of the degree of polymerization. In fact, the G parameter depends on the specifics of the chain composition and on its concentration indeed it is linked to the degree of polymerization. [27] On the contrary, the G value in the high-Q region are of the same order of magnitude: 0.193 ± 0.007 cm^{-1} for monomers, 0.09 ± 0.01 cm^{-1} for oligomers and 0.17 ± 0.03 cm^{-1} for fibrils confirming that in this Q-region we are looking at the same basic unit. The value for the oligomers are about half than those of fibrils and monomers which suggests the adoption of a spherical conformation with a higher density (lower R_g) and a lower degree of polymerization.

Table 1
Fit parameters obtained by using the Becauge model at low Q (Q <0.045 Å^{-1}) and at high Q (0.045 <Q <0.5 Å^{-1}).

	G (cm^{-1})	R_g (Å)	d	bkg (cm^{-1})
low Q				
Monomers	1.30 ± 0.07	253 ± 9	2.8 ± 0.2	0.596 ± 0.006
Oligomers	2.5 ± 0.6	378 ± 41	3.1 ± 0.1	0.371 ± 0.001
Fibrils	12 ± 1	706 ± 52	2.44 ± 0.06	0.570 ± 0.002
high Q				
Monomers	0.19 ± 0.01	10.9 ± 0.4	1.2 ± 0.2	0.43 ± 0.01
Oligomers	0.09 ± 0.01	8.3 ± 0.7	1.3 ± 0.5	0.28 ± 0.01
Fibrils	0.17 ± 0.03	8.4 ± 0.9	1.3 ± 0.6	0.41 ± 0.03

The present results are consistent with previous studies from Dynamic Light Scattering [15] carried out on monomers Aβ_{1-40} and Aβ_{1-42} to study the formation of aggregates over time. Two relaxation times are observed at about 20 and 5000 μs, corresponding to objects with hydrodynamic radii (RH = 1.3 R_g) of about 20 and 5000 Å, respectively. However, the exchanged wave vector regime (and therefore the observable size of the scattering objects) is clearly different between light and neutrons.[15] In the same paper, as already discussed, the authors performed also SANS studies but only on the Aβ_{1-40} and Aβ_{1-42} monomers diluted in dHFIP (deuterated hexafluoroisopropanol) in a Q-region compared with our high-Q region. They also used the Becauge model to fit the data and found for R_g the value of 10 ± 1 Å and 16 ± 1 Å for Aβ_{1-40} and Aβ_{1-42}, respectively. We stress that the value of the hydrodynamic radius for the basic unit that they found in dHFIP is the same of that we found for Aβ_{1-40} incubated in DMSO. However, in their SANS experiments they were not able to see any aggregates (note that they use a smaller wave-vector regime) and to do not enter into details of the structure. For this reason we further treated our SANS data by subtracting the background value obtained by the high Q-fit procedure the signal in order to gain important information about the fractal nature of the structure. Fig. 3 shows the subtracted intensity as a function of Q * RH, after a smoothing of the data, where we considered RH=13 Å, because the mean value of R_g found by using the Becauge model in the corresponding Q-region was approximately 10 Å. The value Q*RH=1 marks the transition between the Guinier and Porod regions, above and below it, respectively. [28] In the Porod region, for Q*RH> 1, it is possible to obtain information about the fractal structure of the system by evaluating the slope of the data in a log–log plot because for Q*RH≫ 1 holds the power law relation: [28]

$$I(Q * RH) \propto (Q * RH)^{-D} \tag{4}$$

In particular, although our analysis is made only over a Q-range that spans less than one order of magnitude, i.e., for $Q * RH > 3$ where the power law holds for the three systems, we evaluated the slope of the data by means of a linear best-fit of $\log[I(Q) - bkg]$ vs. $\log[Q * RH]$. Such analysis is reported in Fig. 3 where we also mark the lower limit (Q*RH=3.5) of the fitting range. We find that the value of D is 1.08 ± 0.04 for monomers that corresponds to an open structure, 1.42 ± 0.05 for oligomers that corresponds to a compacted structure and 1.64 ± 0.08 for fibrils that is close to the so-called Diffusion Limited Cluster–Cluster Aggregation (DLCCA). [28] Although the narrow range used Q is not optimal for investigating the internal structure of such systems, the results give some indications of the aggregating nature of the studied systems.

The SDS–PAGE analysis for Aβ_{1-40} treated with either the oligomer or fibril forming conditions, showed the majority of the peptide as unassembled monomer with a sparse population of minor bands of oligomers and short fibrils. Our results are in accordance with previous reports using gel electrophoresis [18], confirming minor aggregation propensity of Aβ_{1-40}. However, in SDS–PAGE analysis the gel smearing interferes with the ability to identify particular peptide species [16], whereas SANS detections clearly distinguish monomer, oligomer and fibril preparations.

4. Conclusions

The present study examines Aβ_{1-40} peptide in the three aggregation states: monomers, oligomers and fibrils via small angle neutron scattering (SANS) technique. Aβ_{1-40} is suspected to contribute to the neurodegenerative disease processes, such as Alzheimer, through aggregation processes to form soluble oligomers and insoluble fibrils, leading to tissue damage. The Becauge model is used to identify the size of these aggregates via the best fit of the small angle neutron scattering spectra of the three considered systems.

SANS data confirm the results of the SDS/PAGE analysis suggesting in all the three systems the presence of the basic unit (monomer) together with aggregates of increasing molecular weight (and indeed size) going towards the fibril system. In particular, our analysis performed into two different Q-regions reveals that in the high-Q region, the radius Rg of the basic unit, the monomer, is of the order of 10 Å as reported in literature. [11] From the analysis in the low-Q regions, we find that oligomers have dimensions of order of 380 Å corresponding to medium size oligomers whereas fibrils have dimensions of order of 710 Å. Another important parameter is the Guinier scaling factor G in the low-Q region that for monomers is 1.30 ± 0.07 cm^{-1}, for oligomers is 2.5 ± 0.6 cm^{-1} and fibrils is 12 ± 1 cm^{-1} confirming an increase in the size of the scattering object and of the corresponding degree of polymerization. [27] On the contrary, the *G* value in the high-Q region

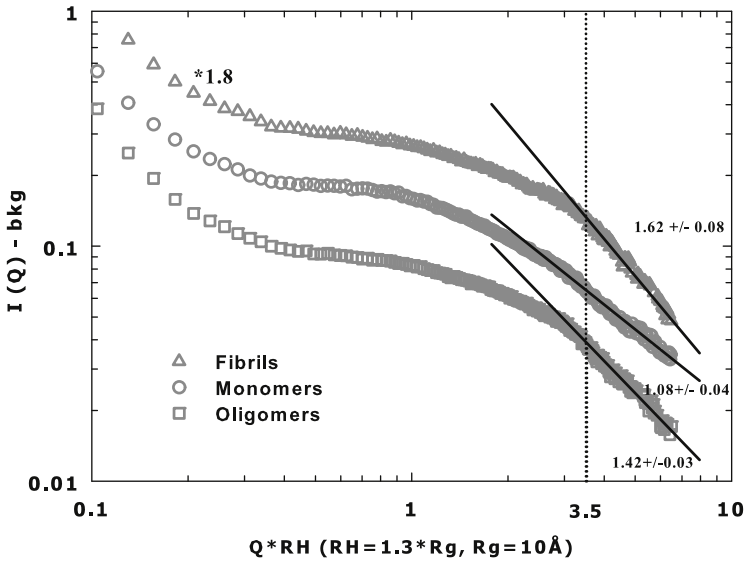

Fig. 3. The subtracted SANS intensity as a function of Q*RH, with RH=13 Å, in a log–log plot. The value Q*RH=1 marks the transition between the Guinier and Porod regions, where we have performed a linear best-fit, for Q*RH$\geq$ 3.5, obtaining indications about the fractal structure of the system, see main text for details. The data of fibrils are multiplied by 1.8 for avoiding points overlap.

is of the same order of magnitude for all three systems: around 0.18 cm^{-1} for fibrils and monomers, and slightly lower at 0.10 cm^{-1} for the oligomers, suggesting a spherical conformation with a higher density (lower R_g) and a lower degree of polymerization.

Finally by analyzing the subtracted intensity vs. Q*RH, where we considered RH=13 Å, and by performing a linear best-fit of $\log[I(Q) - bkg]$ vs. $\log[Q * RH]$ for Q*RH>3, we find that the exponent of the corresponding power law is 1.08 ± 0.04 for monomers that corresponds to an open structure, 1.42 ± 0.05 for oligomers that corresponds to a compacting structure and 1.64 ± 0.08 for fibrils that is close to the so-called Diffusion Limited Cluster–Cluster Aggregation (DLCCA). [28] In conclusion, the results of our SANS study on the aggregation capability of the $A\beta_{1-40}$ peptide are able to discriminate the size and fractal nature of the studied species, clearly characterizing the corresponding aggregation state. In particular we were able to reveal a more open structure for the monomeric system, the only one that was incubated in DMSO.

Acknowledgments

This research is supported by CNR , within the CNR-STFC Agreement 2014–2020 (N. 3420), concerning collaboration in scientific research at the ISIS Spallation Neutron Source. We would like to thank Steve King and Najet Mahmoudi for their support during the measurements and for useful discussions.

References

[1] R. van der Kant, L. Goldstein, Cellular functions of the amyloid precursor protein from development to dementia, Dev. Cell. 32 (4) (2015) 502–515.
[2] P. Spies, M. Verbeek, T. van Groen, J. Claassen, Reviewing reasons for the decreased CSF abeta−42 concentration in Alzheimer disease, Front. Biosci. Landmark Ed. 17 (2012) 2024–3.
[3] P. Tiraboschi, L. Hansen, L. Thal, J. Corey-Bloom, The importance of neuritic plaques and tangles to the development and evolution of AD. neurology, Front. Biosci. Landmark Ed. 62 (11) (2004) 1984–1989.
[4] J. Hardy, D. Selkoe, The amyloid hypothesis of Alzheimer's disease: Progress and problems on the road to therapeutics, Science 297 (2002) 353–356.
[5] J.O. Richard, C.W. Philip, Amyloid precursor protein processing and Alzheimer's disease, Annu. Rev. Neurosci. 34 (2011) 185–204.
[6] L. Hou, H. Shao, Y. Zhang, H. Li, N. Menon, E. Neuhaus, J. Brewer, I. Byeon, D. Ray, M. Vitek, T. Iwashita, R. Makula, A. Przybyla, M. Zagorski, Solution NMR studies of the A beta(1-40) and A beta(1-42) peptides establish that the Met35 oxidation state affects the mechanism of amyloid formation, J. Am. Chem. Soc. 126 (7) (2004) 1992–2005.
[7] M. Friedemann, E. Helk, A. Tiiman, K. Zovo, P. Palumaa, V. Tugu, Effect of methionine−35 oxidation on the aggregation of amyloid-β peptide, Biochem. Biophys. Rep. 3 (2015) 94–99, http://dx.doi.org/10.1016/j.bbrep.2015.07.017.
[8] B. Soreghan, J. Kosmoski, C. Glabe, Surfactant properties of Alzheimer's Abeta peptides and the mechanism of amyloid aggregation, J. Biol. Chem. 269 (46) (1994) 28551–28554.
[9] S. Vivekanandan, J. Brender, S. Lee, A. Ramamoorthy, A partially folded structure of amyloid-beta(1-40) in an aqueous environment, Biochem. Biophys. Res. Commun. 411 (2) (2011) 312–316.
[10] S. Tomaselli, V. Esposito, P. Vangone, N. van Nuland, A. Bonvin, R. Guerrini, T. Tancredi, P.A. Temussi, D. Picone, The alpha-to-beta conformational transition of Alzheimer's Abeta-(1-42) peptide in aqueous media is reversible: A step by step conformational analysis suggests the location of beta conformation seeding, Chembiochem 7 (2) (2006) 257–267.

[11] G. Bitan, M. Kirkitadze, A. Lomakin, S. Vollers, G. Benedek, D. Teplow, Amyloid beta-protein (Abeta) assembly: Abeta 40 and Abeta 42 oligomerize through distinct pathways, Proc. Natl. Acad. Sci. USA 100 (1) (2003) 330–335.
[12] C. Shen, R. Murphy, Solvent effects on self-assembly of 1B-amyloid peptide, Biophys. J. 69 (1995) 640–651.
[13] M. Lee, H. Chang, J. Park, J. Shin, J. Park, J. Choi, J. Kim, S. Na, Conformational changes of Aβ(1-42) monomers in different solvents, J. Mol. Graph. Model. 65 (2016) 8–14.
[14] L. Penazzi, J. Lorengel, F. Sndermann, N. Golovyashkina, S. Marre, C. Mathis, L. Lewejohann, R. Brandt, L. Bakota, DMSO modulates CNS function in a preclinical Alzheimer's disease model, Neuropharmacology 113 (Pt A) (2017) 434–444.
[15] B. Zhang-Haagen, R. Biehl, L. Nagel-Steger, A. Radulescu, D. Richter, D. Willbold, Monomeric amyloid beta peptide in hexafluoroisopropanol detected by small angle neutron scattering, PLoS One 11 (2) (2016) 1–12.
[16] N. Pryor, M. Moss, C. Hestekin, Unraveling the early events of amyloid-β protein (aβ) aggregation: Techniques for the determination of Aβ aggregate size, Int. J. Mol. Sci. 13 (3) (2012) 3038–3072.
[17] R. Pujol-Pina, S. Vilapriny-Pascual, R. Mazzucato, A. Arcella, M. Vilaseca, M. Orozco, N. Carulla, SDS-PAGE analysis of Aβ oligomers is disserving research into Alzheimer's disease: Appealing for ESI-IM-MS, Sci. Rep. 5 (2) (2015) 14809.
[18] K. Dahlgren, A. Manelli, W.J. Stine, L. Baker, G. Krafft, M. LaDu, Oligomeric and fibrillar species of amyloid-beta peptides differentially affect neuronal viability, J. Biol. Chem. 277 (35) (2002) 2046–2053.
[19] G.M. Sancesario, M.T. Cencioni, Z. Esposito, G. Borsellino, M. Nuccetelli, A. Martorana, L. Battistini, R. Sorge, G. Spalletta, D. Ferrazzoli, G. Bernardi, S. Bernardini, G. Sancesario, The load of amyloid-β oligomers is decreased in the cerebrospinal fluid of Alzheimer's disease patients, J. Alzheimers Dis. 31 (4) (2012) 865–878.
[20] G. Sancesario, M. Nuccetelli, A. Cerri, J. Zegeer, C. Severini, M. Ciotti, M. Pieri, A. Martorana, C. Caltagirone, R. Nistico, S. Bernardini, Bromelain degrades Aβ1-42 monomers and soluble aggregates: An in vitro study in cerebrospinal fluid of Alzheimer's disease patients, Curr. Alzheimer Res. 15 (7) (2018) 628–636.
[21] L.A. Feign, D.I. Svergun, Structure Analysis by Small-Angle X-ray and Neutron Scattering, Plenum Press, New York, London.
[22] R. Heenan, S. King, D. Turner, J. Treadgold, SANS2D at the ISIS second target station, in: Proc ICANS-XVII, 2006, pp. 780–785.
[23] R. Heenan, S. Rogers, D. Turner, A. Terry, J. Treadgold, S. King, SANS2D at the second target station, Neutron News 22 (2) (2011) 19–21.
[24] G. Sancesario, Z. Esposito, M. Nuccetelli, S. Bernardini, R. Sorge, A. Martorana, G. Federici, G. Bernardi, G. Sancesario, Abeta1-42 detection in CSF of Alzheimer's desease is influenced by temperature: Indication of reversible abeta1-42 aggregations? Exp. Neurol. 223 (2010) 371–376.
[25] O. Arnold, J.C. Bilheux, J. Borreguero, A. Buts, S. Campbell, L. Chapon, M. Doucet, N. Draper, R.F. Leal, M. Gigg, V. Lynch, A. Markvardsen, D. Mikkelson, R. Mikkelson, R. Miller, K. Palmen, P. Parker, G. Passos, T. Perring, P. Peterson, S. Ren, M. Reuter, A. Savici, J. Taylor, R. Taylor, R. Tolchenov, W. Zhouc, J. Zikovsky, Mantid—data analysis and visualization package for neutron scattering and μsr experiments, Nucl. Instrum. Methods Phys. Res. A 764 (2014) 156–166.
[26] B. Hammouda, Monomeric amyloid beta peptide in hexafluoroisopropanol detected by small angle neutron scattering, J. Appl. Crystallogr. 43 (2010) 1474–1478.
[27] G. Beaucage, Small-angle scattering from polymeric mass fractals of arbitrary mass-fractal dimension, J. Appl. Crystallogr. 29 (1996) 134–146.
[28] S. Magazu, G. Maisano, F. Mallamace, N. Micali, Growth of fractal aggregates in water solutions of macromolecules by light scattering, Phys. Rev. A 39 (8) (1989) 4195–4200.